



# Chemical synthesis and molecular modeling of novel substituted N-1,3-benzoxazol-2-yl benzene sulfonamides as inhibitors of *inhA* enzyme and *Mycobacterium tuberculosis* growth

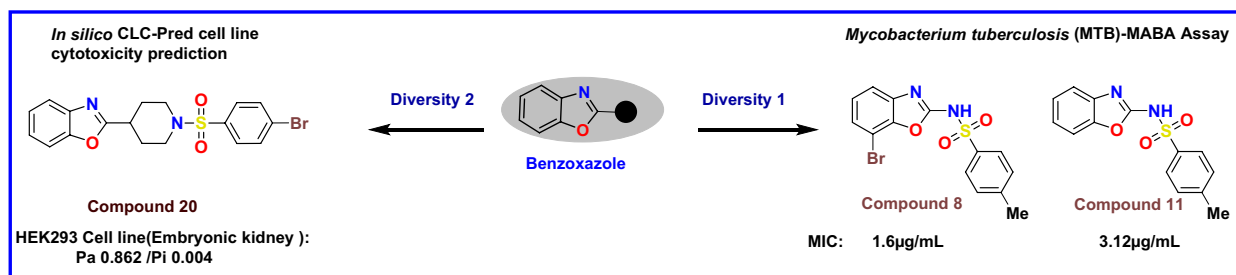
Narendra Singh Chundawat<sup>1</sup> · Gajanan S. Shanbhag<sup>1</sup> · Narendra Pal Singh Chauhan<sup>1</sup>

Received: 30 June 2020 / Accepted: 29 September 2020  
© Iranian Chemical Society 2020

## Abstract

Tuberculosis (TB) is one of the major contagious diseases with high mortality which is caused by *Mycobacterium tuberculosis* (Mtb) pathogen. Due to the existing antibiotic resistance (MDR-TB) to tuberculosis, the demand for the development of new potential chemotherapy drugs is increasing. Herein, we report synthesis of two novel benzoxazole-based series, namely 2-phenyl benzoxazole sulfonamide and 2-piperidine-benzoxazole sulfonamides. These compounds were evaluated for their antimycobacterial activity against *Mycobacterium tuberculosis* H37Rv strain, using the microplate alamarBlue assay. Molecular docking studies were carried out to comprehend the binding mode of the compounds. It is evident from molecular docking studies and minimum inhibitory concentration assay (MIC) that 2-phenyl benzoxazole sulfonamide scaffold has a greater potential of antitubercular activity possibly by ENR inhibition (*inhA* inhibitors). In silico cytotoxicity studies using CLC-Pred tool database suggested that both the series were relatively safe.

## Graphic abstract



**Keywords** *Mycobacterium tuberculosis* · Benzoxazole sulfonamide · Antitubercular activity · *inhA* inhibitors · Molecular docking · Cytotoxicity

## Introduction

Tuberculosis (TB) which is caused by *Mycobacterium tuberculosis* is one of the prime infectious diseases in human beings Bogatcheva et al. [1]. It is responsible for the second highest cause of death for humans following human

immunodeficiency virus/AIDS. Ever since 1993, TB has been recognized as a global health emergency by the World Health Organization. TB causes more than nine million new cases annually with a casualty of about 1.8 million people worldwide every year. In modern era, numerous drugs have emerged, for eradicating TB. However, resistance to those drugs is an alarming matter. Due to recurring incidences of multidrug-resistant (MDR-TB) and extensively drug-resistant (XDR) strains of *M. tuberculosis*, there is a global necessity to develop new age chemotherapeutics to battle different forms of TB Rattan et al. [2].

✉ Gajanan S. Shanbhag  
gajushanbhag@yahoo.com

<sup>1</sup> Department of Chemistry, Bhupal Nobles' University,  
Udaipur, Rajasthan, India

Mycolic acid is a basic component of mycobacterial cell wall present in the FAS (fatty acid synthase) system of human pathogen *M. tuberculosis*. For the survival and pathogenesis of *M. tuberculosis*, "Mycolate biosynthesis" is a key factor. In the biosynthesis of fatty acids Qureshi et al. [3] in *M. tuberculosis*, two distinct enzymes FAS I and II are involved. FAS I is involved in synthesis of the C<sub>26</sub> saturated straight-chain fatty acids to provide branch of the mycolic acids. FAS II will provide the meromycolate backbone by synthesizing C<sub>56</sub> fatty acids. Mycobacterial FAS II utilizes the yields of FAS-I as the primers to expand fatty acyl chain lengths even further Bloch et al. [4], Kikuchi et al. [5]. For type II fatty acid synthase (FAS II), from the *M. tuberculosis*, *inhA*, the enoyl acyl carrier protein reductase (ENR) Maria et al. [6] is the major enzyme which catalyzes the NADH-dependent reduction of trans double bond of acyl carrier protein (2-trans-enoyl-ACP) to yield NAD<sup>+</sup> and reduced enoyl-thioester-ACP substrate, which ultimately contributes to the synthesis of mycolic acid (MA). We could envisage the growing publications on the MTB enoyl-ACP reductase (ENR/*inhA*) enzyme with various O-, N- Desai et al. [7] and azole-containing heterocyclic moieties Martínez-Hoyos et al. [8].

Recent studies suggest that substituted benzoxazoles are of great importance in the medicinal field due to their wide range of pharmaceutical activity. Benzoxazole nucleus is very common motif among heterocyclic compounds exhibiting significant pharmacological activities, especially antimicrobial activities Kamal et al. [9]. Many literature reports suggest that benzoxazole scaffolds have significant biological activities such as antibacterial, antifungal, antiparasitic, antihistaminic, antiviral and anthelmintic activities. Kumar and Kumar [10], Katsura et al. [11], Haugwitz et al. [12], Paget et al. [13], Ozlem et al. [14], Hitesh et al. [15]. Many natural products contain benzoxazole moiety as major component, for example boxazomycin A, nakijinol B (Fig. 1). Recently, Lucie Brulíková et al. [16] published a review on benzoxazole derivatives as promising antitubercular agents. Refer Fig. 1 for representative benzoxazole derivatives as potential antitubercular agents reported recently.

Recent report from Ertan-Bolelli et al. [17] has suggested 5-substituted phenyl sulfonamido benzoxazole derivatives as *inhA* inhibitors. Joshi et al. [18, 19] demonstrated in their study that the *inhA* inhibitor, 1-cyclohexyl-*N*-(3,5-dichlorophenyl)-5-oxopyrrolidine-3-carboxamide (pyrrolidincarboxamide or 641), encompasses three hydrophobic moieties, namely cyclohexyl, oxopyrrolidine, and 3,5-dichlorophenyl, were swapped by the newly designed molecules containing 1,3,4-thiadiazole, pyrrole, and substituted phenyl ring which emulated the interactions of the former groups. These previous reports prompted us to explore the possibility of *inhA* as the target for our newly planned benzoxazole derivatives.

Cell toxicity is characterized by cytotoxicity. Early assessment of the cytotoxicity of potential NCEs is an essential part of the drug discovery, as it could be a potential derailer. Various *in silico* approaches for phenotypic screening are available to reduce the time and cost of *in vivo* experimental screening of cytotoxic agents. Freely available alternatives, such as ChEMBL Gaulton et al. [20] and PubChem Wang et al. [21], are very useful in assessing cytotoxicity data for tumor and normal cell line chemicals. These techniques provide a prospect for the use of these data as a cell line cytotoxicity assessment for newly synthesized compounds.

In our previous study, we have demonstrated that the synthesis and *in vitro* antimicrobial activity of novel substituted *N*-1,3-benzoxazol-2-yl benzene sulfonamides. The present work is based on a ligand-based drug design that uses benzoxazole as its core. To speed up the drug discovery course, the crystallographic 3D structural information of the biomolecular targets offers unbelievable prospect for advancing such novel drug design. To attain this, docking simulation was executed to visualize the binding orientation pattern of small molecules to protein targets to envisage their affinity and activity.

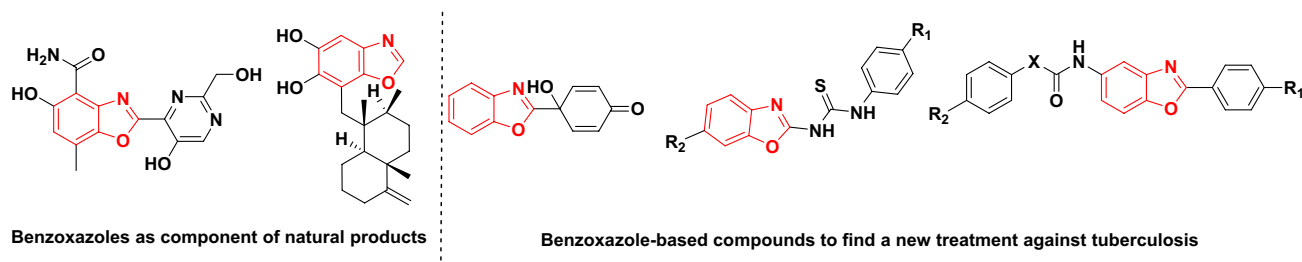


Fig. 1 Representative benzoxazole derivatives as potential antitubercular agents and natural products containing benzoxazole motif

## Results and discussion

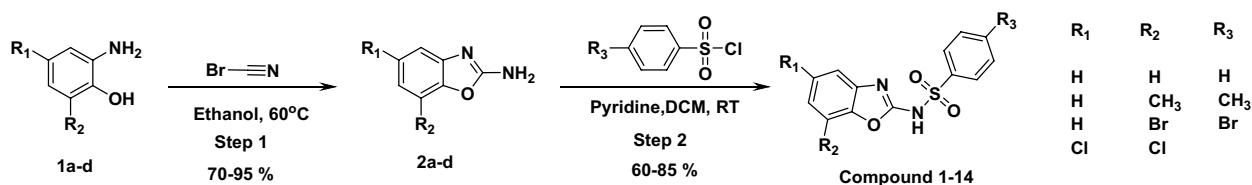
### Chemistry

Synthetic outlines for synthesizing N-1,3-benzoxazol-2-yl benzene sulfonamides (Compounds 1–14) are shown in Schemes 1, and 2-piperidine-1,3-benzoxazole sulfonamides (Compounds 15–20) are synthesized in Scheme 2. These compounds have been characterized by advanced spectral means. Synthesized compound structures using Schemes 1 and 2 were confirmed using  $^1\text{H}$  NMR, IR spectroscopy and mass spectroscopic analysis.

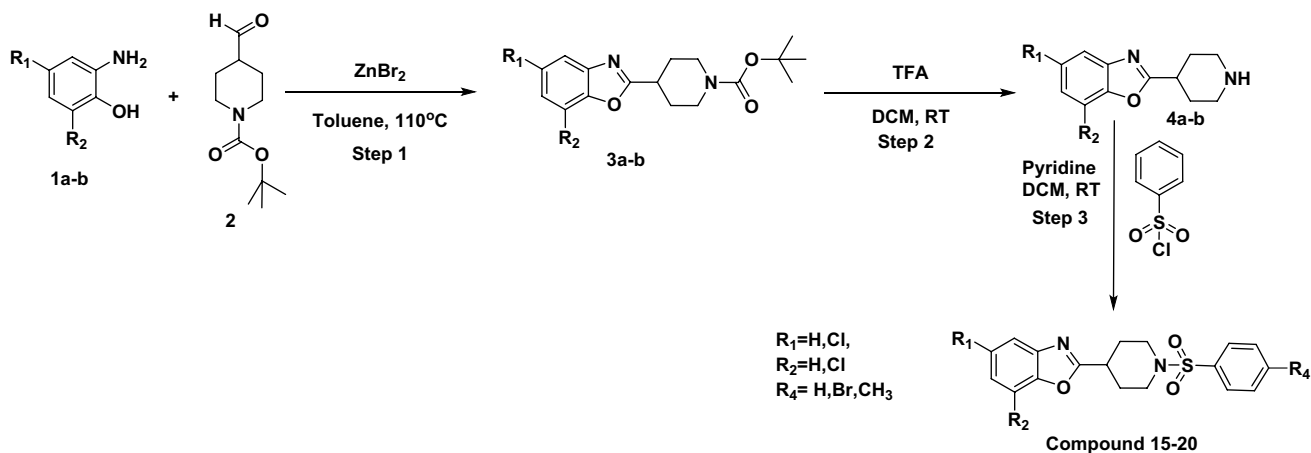
Broad singlet at  $\delta$  12.7 to 13.0 ppm corresponding to one of  $-\text{SO}_2\text{NH}$  ( $\text{D}_2\text{O}$  exchangeable) in  $^1\text{H}$  NMR confirms the formation of benzoxazol-2-yl benzene sulfonamide derivatives (1–14). Structures were further confirmed by IR spectroscopy for the presence of S=O stretch in the range of

1370–1335  $\text{cm}^{-1}$ , N–H stretch 3550–3000  $\text{cm}^{-1}$  and S–N stretch of 925–910  $\text{cm}^{-1}$ .

For the piperidine-benzoxazole sulfonamide derivatives (compounds 15–20),  $^1\text{H}$  NMR confirmed the presence of piperidine ring by showing the peaks in the ranges of  $\delta$  1.70–2.00 ppm (m, 2H), 2.07–2.23 ppm (m, 2H), 2.53–2.60 ppm (m, 2H), 2.90–3.30 ppm (m, 1H) 3.56–3.80 ppm (m, 1H). This was further confirmed by IR spectroscopy by the presence of S=O stretch in the range of 1370–1335  $\text{cm}^{-1}$ , 1195–1168  $\text{cm}^{-1}$  and S–N stretch of 925–910  $\text{cm}^{-1}$ . The presence of the tert-butyl group in its penultimate intermediate (3a–b, refer Scheme 2) was confirmed by singlet obtained at 1.42 ppm. Synthesized compound details along with physical data and corresponding yields are given in Tables 1, 2 (Scheme 1) and Tables 3, 4 (Scheme 2)



**Scheme 1** Synthesis of N-1,3-benzoxazol-2-yl benzene sulfonamides

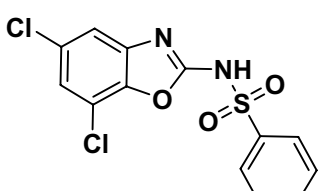
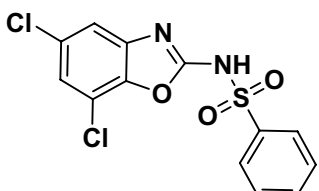
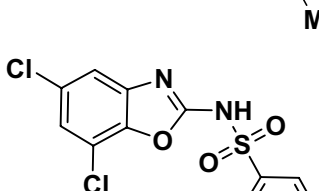
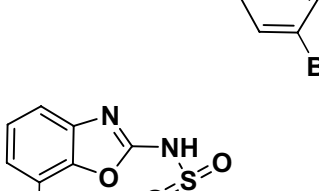
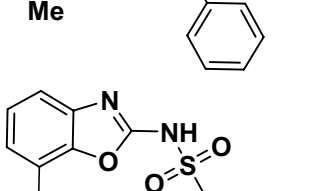
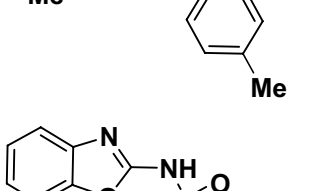


**Scheme 2** Synthesis of 2-piperidine-1,3-benzoxazole sulfonamides

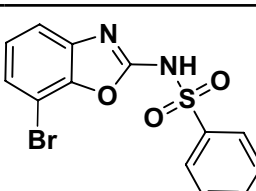
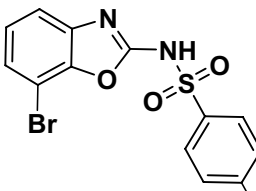
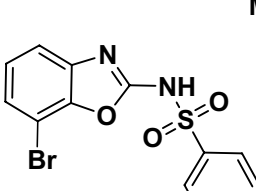
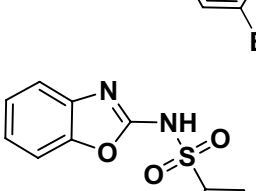
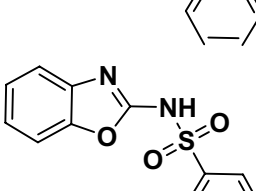
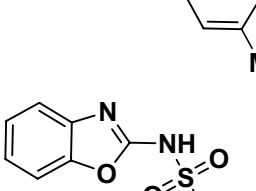
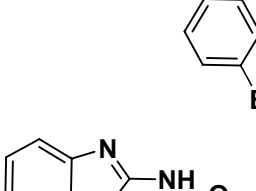
**Table 1** Reaction time and yields for step 1 are given below

Intermediate	R <sub>1</sub>	R <sub>2</sub>	Reaction time (h)	Yield (%)	LCMS characterization
2a	H	H	8	75	MS (ESI): $m/z$ = found 135.14 [ $\text{M}^+$ ]; calcd. 134.05
2b	H	CH <sub>3</sub>	6	80	MS (ESI): $m/z$ = found 149.16 [ $\text{M}^+$ ]; calcd. 148.06
2c	H	Br	10	93	MS (ESI): $m/z$ = found 214.03 [ $\text{M}^+ + 2$ ]; calcd. 211.96
2d	Cl	Cl	12	86	MS (ESI): $m/z$ = found 203.02 [ $\text{M}^+ + 1$ ]; calcd. 201.97

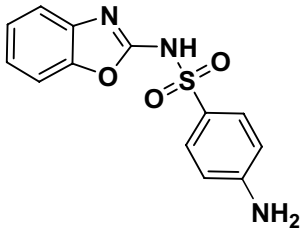
**Table 2** Reaction time and yields for step 2 are given below along with final compound details. Spectral analysis is provided in the Spectral analysis section

Compound no.	Compound structure	Reaction time (h)	Yield (%)
1		2.5	56
2		3	59
3		4	67
4		2.5	60
5		4	69
6		3	66

**Table 2** (continued)

Compound no.	Compound structure	Reaction time (h)	Yield (%)
7		2	69
8		3	60
9		4	70
10*		3	62
11*		3	67
12		2	69
13		3	72

**Table 2** (continued)

Compound no.	Compound structure	Reaction time (h)	Yield (%)
14		4	55

**Table 3** Reaction time and yields for step 1 are given below. Reaction yields for step 2 were quantitative

Intermediate	R <sub>1</sub>	R <sub>2</sub>	Reaction time (h)	Yield (%)	LCMS characterization
3a	H	H	2	70	MS (ESI): <i>m/z</i> = found 303.37 [M <sup>+</sup> ]; calcd. 302.16
3b	Cl	Cl	12	83	MS (ESI): <i>m/z</i> = found 372.26 [M <sup>+</sup> +1]; calcd. 370.09

### In silico molecular docking studies

Docking study of benzene sulfonamide (series 1)- and phenylsulfonyl-piperidine (series 2)-based benzoxazole derivatives:

In order to examine the mechanism of antitubercular activity and to understand intermolecular drug–receptor interactions of the newly synthesized 20 benzoxazole derivatives from both the series, molecular docking studies were executed using the crystal structures of *inhA*, complexed with 1-cyclohexyl-N-(3,5-dichlorophenyl)-5-oxopyrrolidine-3-carboxamide (i.e., PDB ID 4TZK, 1.62 Å X-ray resolution) [22] exercising the Surflex-Dock program of SYBYL-X 2.0 software. Because of the growing resistance to isoniazid [INH] against *inhA*, enoyl acyl carrier protein reductase (ENR) from *M. tuberculosis* was used as an active site for all the inhibitors for docking experiment as shown in Fig. 2a and b. The predicted binding energies of the compounds are recorded in Table 5. The docking study revealed good docking score against *M. tuberculosis* for all the synthesized compounds.

Docking studies with Surflex-Dock assessment have confirmed that the binding patterns of all the synthesized benzoxazole analogues are identical in comparison with the

available *inhA*, NAD<sup>+</sup>, pyrrolidine carboxamide structures He et al. [23]. Benzoxazole derivatives have similar hydrogen-bonding arrangement with the substrate NAD<sup>+</sup> and side chain of Tyr158, which is a part of the enzyme's catalytic residues (Fig. 2a and b).

Two key H-bonding interactions were shown by the pyrrolidinecarboxamide (4TZK ligand). The oxygen atom on the carbonyl group of five-membered ring lactam is connected via hydrogen bond to the hydroxyl group of amino acid residue Tyr158 and to 2'-hydroxyl moiety of the nicotinamide ribose. The lactam ring of the pyrrolidinecarboxamide (4TZK ligand) also interacted with the cofactor NAD<sup>+</sup> (Fig. 5a–c).

We focused our attention on the highly active compounds from series 1, namely compound **8** (MIC of 1.6 µg/mL) and compound **11** (MIC 3.12 µg/mL), for the characteristic receptor–ligand interactions projected by the Surflex-Dock binding mode. In our findings, compounds **8** and **11** displayed a relative type of conformation and orientation as that of standard crystallographic ligand, i.e., pyrrolidinecarboxamide, along with additional hydrogen bonding interactions with surrounding amino acids.

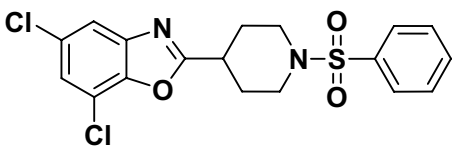
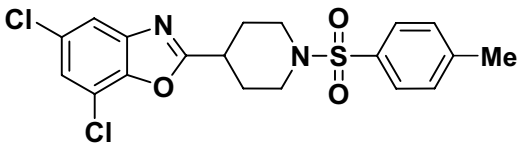
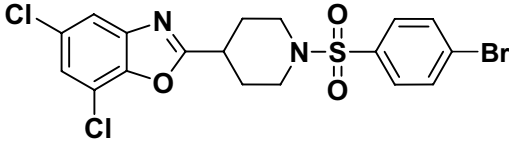
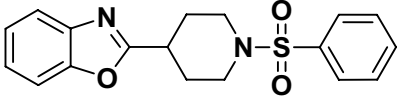
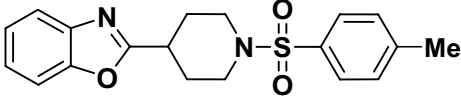
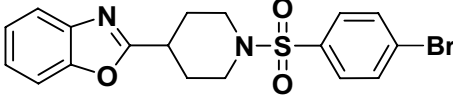
As illustrated in Fig. 3a–c, at the enoyl acyl carrier protein reductase (ENR) enzyme (PDB ID: 4TZK) active site, the benzoxazole Sulfonamide compound **8** makes the three key hydrogen bonding interactions. Among these three interactions, benzoxazole ring nitrogen (N) atom formed two hydrogen bonding interactions, one with the co-factor NAD<sup>+</sup> (2.33 Å) and other with TYR158 (2.32 Å). Another hydrogen bonding interaction rose from the hydrogen atom of NH of sulfonamide group (SO<sub>2</sub>NH), with oxygen atom of TYR158 (2.48 Å).

As depicted in Fig. 4a–c, in the active site of the enoyl acyl carrier protein reductase (ENR) enzyme (PDB ID: 4TZK), compound **11** also demonstrated the similar binding pattern with three key hydrogen bonding interactions. Among those, two interactions are coming from the nitrogen atom (N) of the benzoxazole ring with the hydrogen atoms of NAD<sup>+</sup> (2.37 Å) and TYR158 (2.34 Å). Remaining hydrogen bonding interaction outstretched from the hydrogen atom of N–H of sulfonamide group (SO<sub>2</sub>NH) with oxygen atom of TYR158 (2.50 Å).

Overall outcome of the docking studies using Surflex-Dock revealed that all the synthesized compounds engaged the similar binding interactions as those of pyrrolidinecarboxamide derivative (Fig. 5).

Figure 6a, b represents the other hydrophilic and hydrophobic amino acids surrounded by the studied compounds **8** & **11**.

**Table 4** Reaction time and yields for step 3 are given along with final compound details below

Compound no.	Compound structure	Reaction time (h)	Yield (%)
15		2	63
16		3	67
17		4	68
18		3	68
19		3	69
20		2	80

Spectral analysis is shown in the Spectral analysis section

**Fig. 2** Docked view of all the compounds at the active site of the enzyme PDB ID: 4TZK

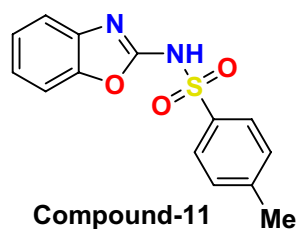
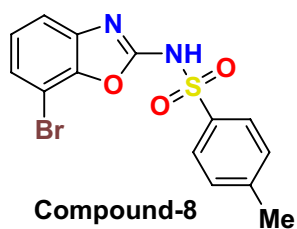
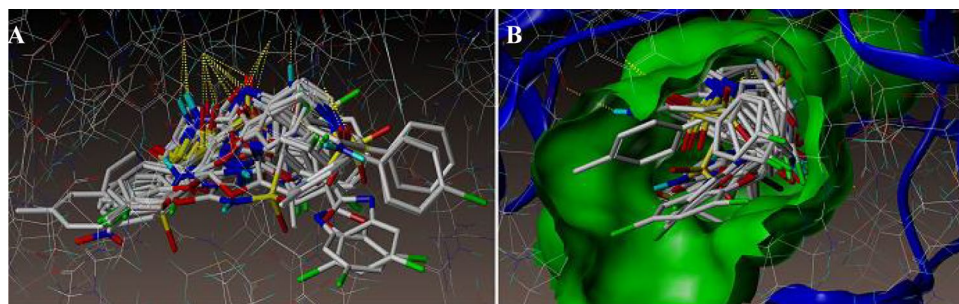




**Table 5** Surfex Docking score (kcal/mol) of the benzoxazole derivatives

Compounds	C score <sup>a</sup>	Crash score <sup>b</sup>	Polar score <sup>c</sup>	D score <sup>d</sup>	PMF score <sup>e</sup>	G score <sup>f</sup>	Chem score <sup>g</sup>
4TZK ligand	8.73	-1.39	1.18	-168.11	-49.19	-285.29	-37.47
19	6.94	-1.04	0.11	-106.075	-44.224	-262.286	-32.535
8	6.77	-1.49	0.98	-103.226	-49.423	-243.558	-32.250
11	6.29	-1.03	0.98	-89.633	-54.975	-220.471	-30.480
18	6.18	-0.81	0.66	-90.276	-57.459	-228.287	-30.226
13	5.97	-0.82	0.95	-93.268	-57.501	-214.938	-28.347
20	5.76	-0.87	1.06	-92.905	-58.247	-221.634	-32.385
15	5.35	-1.71	0.47	-111.421	-58.163	-262.986	-33.821
9	5.26	-0.68	0.74	-99.342	-49.206	-200.760	-30.075
14	5.23	-1.57	1.38	-75.614	-43.630	-204.957	-31.873
16	5.19	-0.85	0.62	-93.250	-57.971	-215.132	-32.988
6	5.17	-0.82	0.66	-96.735	-46.708	-205.388	-29.770
17	4.99	-0.79	0.61	-97.764	-49.148	-217.801	-30.921
12	4.91	-1.40	1.06	-89.627	-54.161	-200.000	-30.145
10	4.90	-2.72	1.11	-92.221	-45.364	-227.320	-30.666
7	4.61	-0.78	0.04	-96.986	-53.485	-194.166	-27.674
5	4.53	-1.98	0.00	-103.641	-43.298	-213.708	-29.488
1	4.13	-2.01	1.12	-101.788	-58.955	-234.130	-30.815
4	4.06	-1.15	0.00	-89.580	-36.472	-183.882	-29.195
2	3.61	-0.76	0.52	-89.695	-48.189	-181.627	-29.795
3	3.07	-0.90	0.68	-93.992	-50.518	-183.842	-30.201

<sup>a</sup>C Score (Consensus Score) integrates a number of popular scoring functions for ranking the affinity of ligands bound to the active site of a receptor and reports the output of total score

<sup>b</sup>Crash score reveals the inappropriate penetration into the binding site. Crash scores close to 0 are favorable. Negative numbers indicate penetration

<sup>c</sup>Polar indicates the contribution of the polar interactions to the total score. The polar score may be useful for excluding docking results that make no hydrogen bonds

<sup>d</sup>D score for charge and van der Waals interactions between the protein and the ligand

<sup>e</sup>PMF score indicates the Helmholtz free energies of interactions for protein–ligand atom pairs (potential of mean force, PMF)

<sup>f</sup>G score shows hydrogen bonding, complex (ligand–protein) and internal (ligand–ligand) energies

<sup>g</sup>Chem-score points for H-bonding, lipophilic contact and rotational entropy, along with an intercept term

The scoring functions, viz. C Score, Crash Score, Polar Score, D Score, PMF Score, Chem Score, G Score, from the Surfex-Dock are shown in Table 5 to understand the binding affinity between benzoxazole derivatives and the ENR protein receptor.

All the compounds displayed a Consensus Score (C Score) in the range of 7.00–3.07, signifying the summary of all forces of interaction between the ligands and the enoyl acyl carrier protein reductase (ENR) *inhA*. Helmholtz free energies of interactions for protein–ligands atom pairs ranged from 45 to 50. Electrostatic and van der Waals interactions between the protein and benzoxazole hits were found around 100. Compounds H-bonding, complex (ligand–protein) and internal (ligand–ligand) energies are around 250. These scores indicate that the molecules preferably bind to the enoyl acyl carrier protein reductase (ENR) *inhA* enzyme

compared to the reference ligand reference 4TZK ligand (pyrrolidinecarboxamide). Compounds from both the series are efficiently binding to the substrate (ligand) binding site of ENR. Ligand–receptor complex was stabilized by the key H-bonding interactions with cofactor NAD<sup>+</sup> and Tyr158, along with additional surrounding hydrophobic and hydrophilic amino acid residues. These observations conclude that these benzoxazole sulfonamide derivatives are tight binders of the ENR and can be further developed as the superior ENR inhibitors. Rational correlation between predicted and experimental results was established for the synthesized compounds. With this, we conclude that the molecular docking with the support of in vitro assay confirmation could serve as an efficient preselection method for recognizing new enoyl acyl carrier protein reductase (ENR) inhibitors.

**Fig. 3** Docked view of compound **8** at the active site of the enzyme PDB: 4TZK

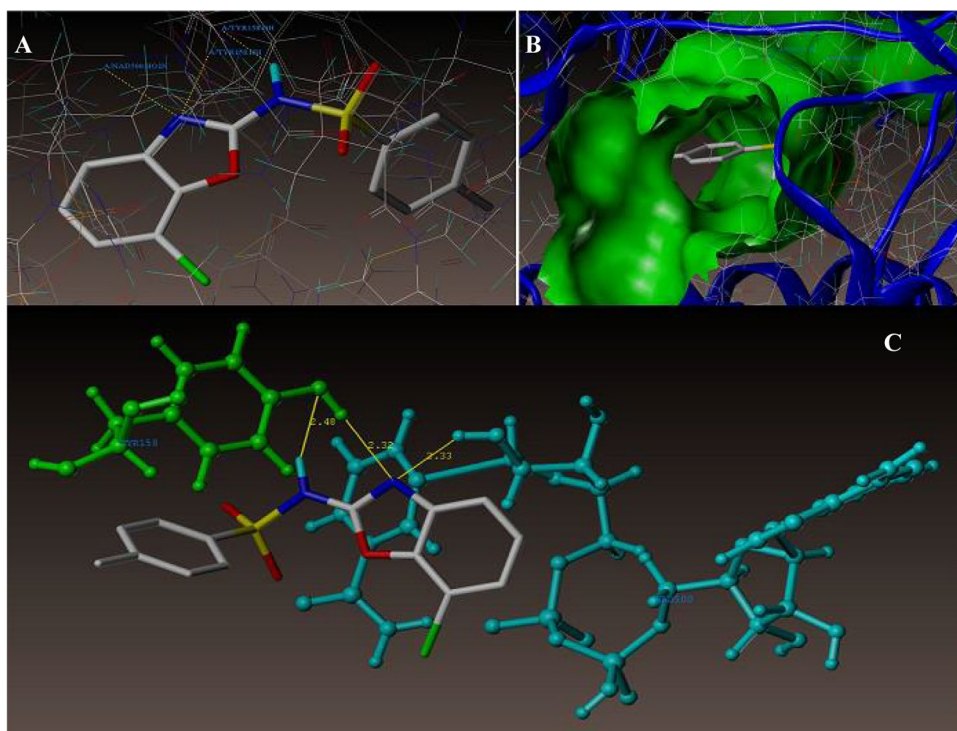
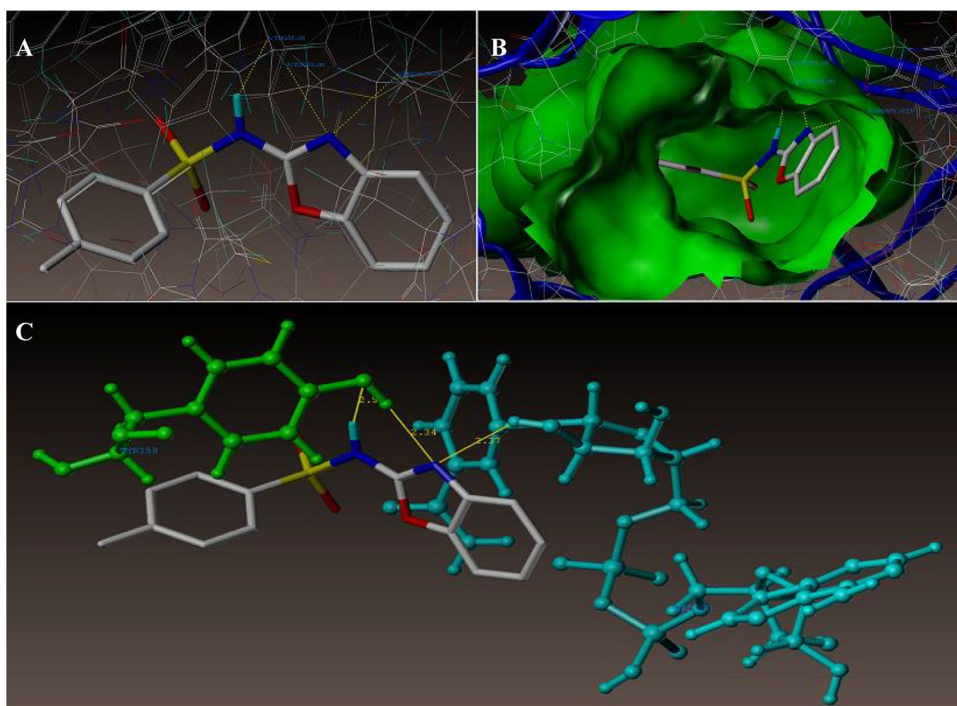


**Fig. 4** Interaction of compound **11** at the binding site of the enzyme (PDB ID: 4TZK)



## Biology

### Antimycobacterial Activity

In vitro evaluation of compounds for antimycobacterial activity against *M. tuberculosis* H37Rv was performed using

microplate alamarBlue assay (MABA) technique with ciprofloxacin, pyrazinamide and streptomycin as the internal standards. All the synthesized compounds exhibited significant, moderate even negligible activity at different concentrations. Among all the assessed molecules, compound **8** from Scheme 1 was exceptionally active with the MIC of



**Fig. 5** **a** Docked mode of 4TZK\_ligand; **b** Inside the proposed binding pocket of InhA; **c** 3D docked view of the 4TZK\_ligand. Binding site residues; red-colored Try158 amino acid, blue-colored cofactor NAD<sup>+</sup>; the molecule is colored according to atom type

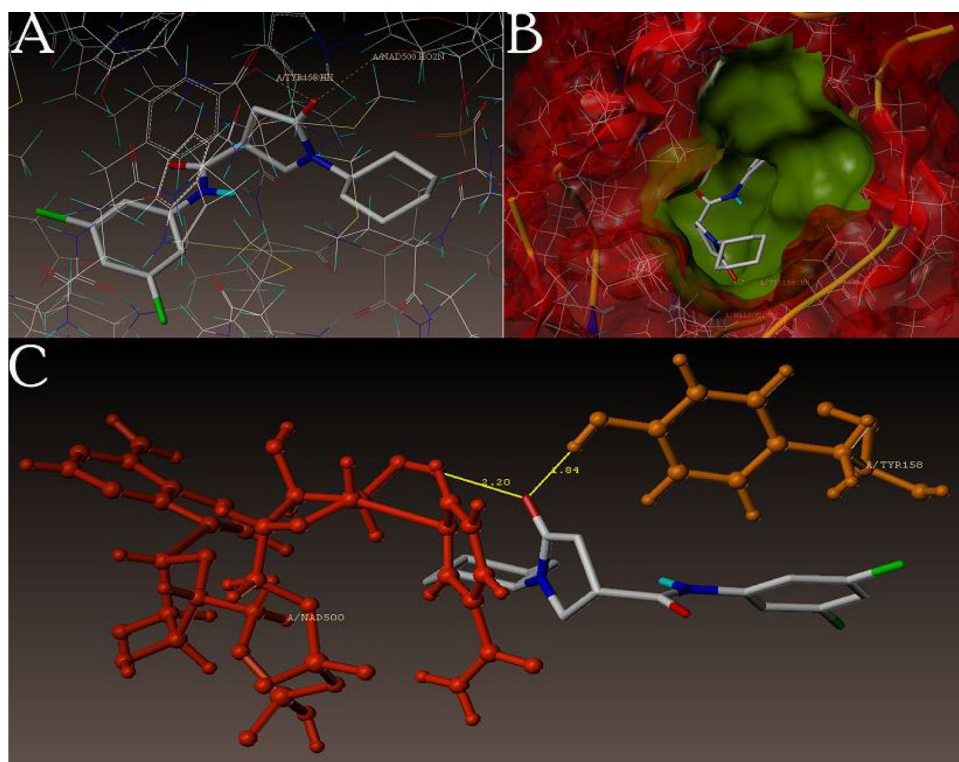
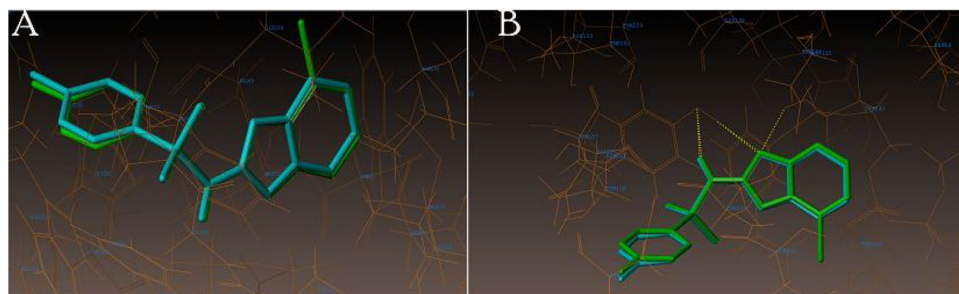


**Fig. 6** **a** Hydrophobic amino acids surrounded to compounds **8** (green color) and **11** (cyan color). **b** Hydrophilic amino acids surrounded to compounds **8** and **11**



1.6 µg/mL, followed by compound **11** from Scheme 1 with 3.12 µg/mL. The present study suggested that the structural substitution of synthesized compounds could have better impact on changing the efficacy of antimycobacterial activity when further screened for MIC.

## Human cell line cytotoxicity (in silico Model)

### In silico prediction of benzoxazole derivatives

All the 20 benzoxazole derivatives from both the series were selected and taken for cytotoxicity prediction in different cell lines by making use of CLC-Pred tool Lagunin et al. [24]. Almost all the compounds from the phenyl sulfonamide benzoxazole series showed aspirated outcome of probability of being lesser cytotoxic to any of the mentioned

cell lines. Compounds from piperidine-based benzoxazole series specifically target the HEK293 cell line, which is present in human embryonic kidney. We strongly believe that piperidine-based benzoxazole type of compounds may be the best starting points for renal fibroblasts and myofibroblasts of Chronic Kidney cancer research. Compilation of cell line toxicity study results is shown in Table 6.

## Conclusion

In the present study, we have developed a novel benzoxazole sulfonamide-based chemical series, which can be developed as possible antitubercular agents. Two distinct benzoxazole sulfonamide scaffolds were synthesized and evaluated for their antimycobacterial potential. Among all, N-phenyl benzoxazole compounds, **8** (N-(7-bromobenzo[d]

oxazol-2-yl)-4-methylbenzenesulfonamide) and **11** (N-(benzo[d]oxazol-2-yl)-4-methylbenzenesulfonamide) showed prominent antimycobacterial activities. Utilizing *In-silico* ligand- and structure-based approaches, we have successfully demonstrated the preferential binding of these benzoxazole derivatives to *inhA* protein, which was further supported by the biochemical *M. tuberculosis* inhibition assay. Cytotoxicity profile prediction, using the CLC-Pred tool, indicated cleaner profile for N-phenyl benzoxazole compounds. Piperidine-based benzoxazole compounds are specifically active in embryonic human kidney HEK293 cell line. In conclusion, we believe that phenyl benzoxazole sulfonamide compounds can be developed as new lead antitubercular agents with preferential binding to the enoyl acyl carrier protein reductase (ENR) enzyme. Benzoxazole-based piperidine compounds may also be an appropriate chemotype for kidney cancer research.

## Materials and methods

### Experimental

All reagents and solvents for the present study were purchased from commercial sources and used without purification. Both  $^1\text{H}$  and proton-decoupled  $^{13}\text{C}$  spectra were recorded on Bruker Supercon Magnet Avance DRX-300 with 300 MHz and 50 MHz spectrometer, in deuterated solvents with TMS as an internal reference. Chemical shifts  $\delta$  were given in ppm and coupling constant  $J$  in Hz. Multiplicities obtained in NMR spectra are reported as follows: singlet (s), doublet (d), triplet (t), multiplet (m) and broad singlet (br s). IR spectra were recorded using the PerkinElmer BX series FTIR 5000 spectrometer using KBr pellet (Vector-22, Bruker, France). Mass spectra were recorded on 70 eV on VG-Micromass 7070H spectrometer, and elemental analysis was carried out using FLASH EA 1112 CHN analyzer (Thermo finnigan, Italy). Progress of the reactions was monitored by thin-layer chromatography (TLC) on precoated silica gel plates using UV light as a visualizing agent. All the compounds were purified by either recrystallization using suitable solvents or performing column chromatography over Merck silica gel (230–400 flash). Melting points were measured on an open capillary tube in melting point apparatus and are uncorrected. All compounds have been characterized by TLC,  $^1\text{H}$  NMR, MS and IR spectroscopy.

### General procedures and spectral data

Synthetic outlines are shown in Scheme 1.

Step 1: Synthesis of 1, 3-benzoxazol-2-amines (2a-d)

To a stirred solution of substituted 1 mmol of amino phenol (1a–d) in 20 ml of ethanol, a 3 mmol of cyanogen bromide has been added slowly at room temperature. Reaction mixture was heated to 60 °C for 12 h. The reaction was monitored by TLC. After the disappearance of starting material (1a–d), reaction mass was evaporated and the residue was treated with aqueous sodium bicarbonate solution (20 mL) till pH of 8. Solid obtained was filtered and recrystallized with ethanol. The yields obtained ranged from 70 to 90%.

Step 2: Synthesis of N-1,3-benzoxazol-2yl benzene sulfonamides (Compounds 1–14)

Sulfonyl chloride (1.1 mmol) has been added to a stirred solution of 1 mmol step 1 product (benzo[d]oxazol-2-amine) in dry DCM and 10 mmol pyridine. The reaction mixture has been stirred at room temperature for 1–4 h. Reaction was monitored by TLC. After the disappearance of the starting material (2a–d), reaction mass was evaporated under vacuum. Residue obtained was treated with water, to obtain a solid which was purified either by recrystallization using ethyl alcohol or by column chromatography (eluent: ethyl acetate/hexane, 3:7). The yields obtained during the transformation ranged between 54 and 75%.

A total of 14 sulfonamides and four intermediates were prepared, and the details of the compounds **1–15** are given in Tables 1 and 2.

Synthetic outlines are shown in Scheme 2.

Step 1: Synthesis of substituted tert-butyl 4-(benzo[d]oxazol-2-yl)piperidine-1-carboxylate (3a-b)

To a mixed solution of piperidine aldehyde **2** (1.1 mmol) and o-aminophenol 1a-b (1.0 mmol) in 10 mL of toluene, zinc bromide (0.01 mmol) catalyst has been added. The reaction mixture was stirred for 2 h at 111 °C. Reaction was monitored by TLC. Upon completion of the reaction, the reaction mixture was filtered through the Celite bed. The catalyst was washed with ethyl acetate. Solvent was removed under vacuum, and the residue was purified either by recrystallization or by the use of column chromatography to isolate the pure compound. The yields obtained were between 70 and 85%.

Step 2: Synthesis of 2-(piperidin-4-yl)benzo[d]oxazole (4a–b)

To a stirred solution of 1 mmol of substituted tert-butyl 4-(benzo[d]oxazol-2-yl)piperidine-1-carboxylate (3a–b) was added DCM, trifluoroacetic acid (TFA) (40 eq) was added and the reaction mass was stirred at RT for 2 h. TLC showed the absence of starting material. The reaction mass was evaporated in order to obtain a crude product which was taken directly for the next step without further workup.

**Table 6** In silico CLC-Pred cell line cytotoxicity prediction of benzoxazole derivatives from the study area

S. no	Compound name	Cell line	Cell line model type	Affecting parts	Tumor type	Pa	Pi
1	N-(5,7-dichlorobenzo[d]oxazol-2-yl)benzenesulfonamide	HT-29	Colon adenocarcinoma	Colon	Adenocarcinoma	0.465	0.039
		HeLa	Cervical adenocarcinoma	Cervix	Adenocarcinoma	0.421	0.036
		T47D	Breast carcinoma	Breast	Carcinoma	0.374	0.040
		5637	Urothelial bladder carcinoma	Urinary tract	Carcinoma	0.338	0.017
2	N-(5,7-dichlorobenzo[d]oxazol-2-yl)-4-methylbenzenesulfonamide	Hs 683	Oligodendroglioma	Brain	Glioma	0.410	0.110
		CCRF-CEM	Childhood T acute lymphoblastic leukemia	Blood	Leukemia	0.488	0.015
		HT-29	Colon adenocarcinoma	Colon	Adenocarcinoma	0.402	0.057
		HeLa	Cervical adenocarcinoma	Cervix	Adenocarcinoma	0.378	0.046
		5637	Urothelial bladder carcinoma	Urinary tract	Carcinoma	0.333	0.022
		C8166	Leukemic T cells	Blood	Leukemia	0.319	0.039
		T47D	Breast carcinoma	Breast	Carcinoma	0.327	0.056
		Hs 683	Oligodendroglioma	Brain	Glioma	0.323	0.190
3	4-bromo-N-(5,7-dichlorobenzo[d]oxazol-2-yl)benzenesulfonamide	HEK293	Embryonic kidney	Kidney	fibroblast	0.494	0.024
		CCRF-CEM	Childhood T acute lymphoblastic leukemia	Blood	Leukemia	0.469	0.017
		HeLa	Cervical adenocarcinoma	Cervix	Adenocarcinoma	0.380	0.045
		HT-29	Colon adenocarcinoma	Colon	Adenocarcinoma	0.335	0.086
4	N-(7-methylbenzo[d]oxazol-2-yl)benzenesulfonamide	T47D	Breast carcinoma	Breast	Carcinoma	0.304	0.066
		ACHN	Papillary renal	Kidney	carcinoma	0.486	0.014
		C8166	Leukemic T cells	Blood	Leukemia	0.454	0.003
		5637	Urothelial bladder carcinoma	Urinary tract	Carcinoma	0.443	0.003
		G-361	Melanoma	Skin	Melanoma	0.421	0.004
		Raji	B-lymphoblastic cells	Hematopoietic and lymphoid tissue	Leukemia	0.342	0.014
		NCI-H522	Nonsmall cell lung carcinoma	Lung	Carcinoma	0.332	0.055
		MCF7	Breast carcinoma	Breast	Carcinoma	0.334	0.118
5	4-methyl-N-(7-methylbenzo[d]oxazol-2-yl)benzenesulfonamide	HEK293	Embryonic kidney fibroblast	Kidney	fibroblast	0.473	0.026
		ACHN	Papillary renal	Kidney	carcinoma	0.476	0.015
		C8166	Leukemic T cells	Blood	Leukemia	0.450	0.003
		5637	Urothelial bladder carcinoma	Urinary tract	Carcinoma	0.439	0.003
		G-361	Melanoma	Skin	Melanoma	0.415	0.004
		Raji	B-lymphoblastic cells	Hematopoietic and lymphoid tissue	Leukemia	0.339	0.014
		NCI-H522	Nonsmall cell lung carcinoma	Lung	Carcinoma	0.324	0.060
		HEK293	Embryonic kidney fibroblast	Kidney	fibroblast	0.485	0.024
6	4-bromo-N-(7-methylbenzo[d]oxazol-2-yl)benzenesulfonamide	ACHN	Papillary renal	Kidney	carcinoma	0.439	0.021
		C8166	Leukemic T cells	Blood	Leukemia	0.419	0.003

**Table 6** (continued)

S. no	Compound name	Cell line	Cell line model type	Affecting parts	Tumor type	Pa	Pi
7	N-(7-bromobenzo[d]oxazol-2-yl)benzenesulfonamide	5637	Urothelial bladder carcinoma	Urinary tract	Carcinoma	0.410	0.004
		G-361	Melanoma	Skin	Melanoma	0.387	0.004
		Raji	B-lymphoblastic cells	Hematopoietic and lymphoid tissue	Leukemia	0.304	0.023
		MCF7	Breast carcinoma	Breast	Carcinoma	0.362	0.102
		HT-29	Colon adenocarcinoma	Colon	Adenocarcinoma	0.466	0.039
		T47D	Breast carcinoma	Breast	Carcinoma	0.413	0.031
8	N-(7-bromobenzo[d]oxazol-2-yl)-4-methylbenzenesulfonamide	5637	Urothelial bladder carcinoma	Urinary tract	Carcinoma	0.310	0.049
		C8166	Leukemic T cells	Blood	Leukemia	0.310	0.054
		CCRF-CEM	Childhood T acute lymphoblastic leukemia	Blood	Leukemia	0.484	0.016
		HeLa	Cervical adenocarcinoma	Cervix	Adenocarcinoma	0.454	0.030
		HT-29	Colon adenocarcinoma	Colon	Adenocarcinoma	0.390	0.061
		T47D	Breast carcinoma	Breast	Carcinoma	0.355	0.046
9	4-bromo-N-(7-bromobenzo[d]oxazol-2-yl)benzenesulfonamide	C8166	Leukemic T cells	Blood	Leukemia	0.312	0.050
		5637	Urothelial bladder carcinoma	Urinary tract	Carcinoma	0.308	0.053
		HT-29	Colon adenocarcinoma	Colon	Adenocarcinoma	0.433	0.048
10	N-(benzo[d]oxazol-2-yl)benzenesulfonamide	T47D	Breast carcinoma	Breast	Carcinoma	0.377	0.039
		C8166	Leukemic T cells	Blood	Leukemia	0.302	0.069
		5637	Urothelial bladder carcinoma	Urinary tract	Carcinoma	0.382	0.005
		C8166	Leukemic T cells	Blood	Leukemia	0.372	0.005
11	N-(benzo[d]oxazol-2-yl)-4-methylbenzenesulfonamide	G-361	Melanoma	Skin	Melanoma	0.304	0.017
		YAPC	Pancreatic carcinoma	Pancreas	Carcinoma	0.380	0.130
		Hs 683	Oligodendroglioma	Brain	Glioma	0.350	0.161
		5637	Urothelial bladder carcinoma	Urinary tract	Carcinoma	0.370	0.005
		C8166	Leukemic T cells	Blood	Leukemia	0.364	0.006
12	N-(benzo[d]oxazol-2-yl)-4-bromobenzenesulfonamide	YAPC	Pancreatic carcinoma	Pancreas	Carcinoma	0.367	0.151
		A2058	Melanoma	Skin	Melanoma	0.303	0.148
		C8166	Leukemic T cells	Blood	Leukemia	0.348	0.011
13	N-(benzo[d]oxazol-2-yl)-4-nitrobenzenesulfonamide	5637	Urothelial bladder carcinoma	Urinary tract	Carcinoma	0.348	0.012
		YAPC	Pancreatic carcinoma	Pancreas	Carcinoma	0.454	0.029
		5637	Urothelial bladder carcinoma	Urinary tract	Carcinoma	0.388	0.004
		C8166	Leukemic T cells	Blood	Leukemia	0.364	0.006
14	4-amino-N-(benzo[d]oxazol-2-yl)benzenesulfonamide	U-266	Plasma cell myeloma	Blood	Myeloma	0.317	0.112
		RKO	Colon carcinoma	Colon	Carcinoma	0.310	0.140
		5637	Urothelial bladder carcinoma	Urinary tract	Carcinoma	0.370	0.005
		5637	Urothelial bladder carcinoma	Urinary tract	Carcinoma	0.370	0.005

**Table 6** (continued)

S. no	Compound name	Cell line	Cell line model type	Affecting parts	Tumor type	Pa	Pi
		C8166	Leukemic T cells	Blood	Leukemia	0.363	0.006
		MOLT-4	Acute T-lymphoblastic leukemia	Blood	Leukemia	0.316	0.074
		YAPC	Pancreatic carcinoma	Pancreas	Carcinoma	0.369	0.148
		U-266	Plasma cell myeloma	Blood	Myeloma	0.303	0.135
15	5,7-dichloro-2-(1-(phenylsulfonyl)piperidin-4-yl)benzo[d]oxazole	Hs 683	Oligodendroglioma	Brain	Glioma	0.311	0.204
16	5,7-dichloro-2-(1-(phenylsulfonyl)piperidin-4-yl)benzo[d]oxazole	HEK293	Embryonic kidney	Kidney	Fibroblast	0.764	0.005
17	2-(1-((4-bromophenyl)sulfonyl)piperidin-4-yl)-5,7-dichlorobenzo[d]oxazole	HEK293	Embryonic kidney	Kidney	Fibroblast	0.789	0.005
18	2-(1-(phenylsulfonyl)piperidin-4-yl)benzo[d]oxazole	HEK293	Embryonic kidney	Kidney	Fibroblast	0.790	0.005
19	2-(1-tosylpiperidin-4-yl)benzo[d]oxazole	HEK293	Embryonic kidney	Kidney	Fibroblast	0.823	0.005
20	2-(1-((4-bromophenyl)sulfonyl)piperidin-4-yl)benzo[d]oxazole	HEK293	Embryonic kidney	Kidney	Fibroblast	0.862	0.004

Step 3: Synthesis of 2-piperidine-1,3-benzoxazole sulfonamides (Compound 15–20)

Sulfonyl chloride (1.1 mmol) has been added to a stirred solution of 1 mmol step 2 product (2-(piperidin-4-yl)benzo[d]oxazole) in dry DCM and 10 mmol pyridine. The reaction mixture has been stirred at room temperature for 1–4 h. The reaction mass was evaporated under vacuum, after the disappearance of the starting material (4a–b). Residue obtained was treated with water to obtain a solid that was purified either by recrystallization with ethyl alcohol or by column chromatography (eluent: ethyl acetate/hexane, 4:6). The yields obtained during the transformation ranged between 60 and 80%.

A total of six piperidine-based sulfonamides were prepared, and the details of the compounds (15–20) are listed in Tables 2 and 3.

### Spectral analysis of all the synthesized compounds

#### N-5,7-dichlorobenzo[d]oxazol-2-yl)benzene sulfonamide (1)

Yield (%): 56; white semisolid; m.p.:187–189 °C; Rf: 0.62 (ethyl acetate/hexane, 5:5); IR (KBr,  $\text{cm}^{-1}$ ): 3145  $\text{cm}^{-1}$  (Ar–H stretching), 1620, 1400  $\text{cm}^{-1}$  (benzoxazole stretching), 1370, 1120  $\text{cm}^{-1}$  ( $-\text{SO}_2-\text{NH}-$  stretching), 920  $\text{cm}^{-1}$  (S–N stretch), 850 (C–Cl stretching);  $^1\text{H-NMR}$  (300 MHz,

DMSO  $d_6$ ):  $\delta$  7.32 (d, 1H, Ar–H), 7.52–7.54 (m, 2H, Ar–H), 7.62–7.64 (m, 1H, Ar–H), 7.72–7.74 (m, 2H, Ar–H), 7.79 (d, 1H, Ar–H), 12.7 (s, 1H,  $1 \times \text{NH}$ ); MS (ESI):  $m/z$  = found 342.96 [ $\text{M}^+ + 1$ ]; calcd. 341.96.

#### N-(5,7-dichlorobenzo[d]oxazol-2-yl)-4-methylbenzenesulfonamide (2)

Yield (%): 59; white solid; m.p.:194–198 °C; Rf: 0.52 (ethyl acetate/hexane, 5:5); IR (KBr,  $\text{cm}^{-1}$ ): 3140  $\text{cm}^{-1}$  (Ar–H stretching), 1630, 1410  $\text{cm}^{-1}$  (benzoxazole stretching), 1380, 1160  $\text{cm}^{-1}$  ( $-\text{SO}_2-\text{NH}-$  stretching), 925  $\text{cm}^{-1}$  (S–N stretch), 860 (C–Cl stretching);  $^1\text{H NMR}$  (300 MHz, DMSO  $d_6$ ):  $\delta$  2.33 (s, 3H,  $1 \times \text{CH}_3$ ), 7.29–7.35 (m, 3H, Ar–H), 7.71 (ddd, 2H Ar–H), 7.79 (1H, Ar–H), 12.8 (s, 1H,  $1 \times \text{NH}$ ). MS (ESI):  $m/z$  = found 357.86 [ $\text{M}^+ + 1$ ]; calcd. 355.98.

#### 4-bromo-N-(5,7-dichlorobenzo[d]oxazol-2-yl)benzene sulfonamide (3)

Yield (%): 67; gray solid; m.p.:184–188 °C; Rf: 0.62 (ethyl acetate/hexane, 5:5); IR (KBr,  $\text{cm}^{-1}$ ): 3145  $\text{cm}^{-1}$  (Ar–H stretching), 1620, 1430  $\text{cm}^{-1}$  (benzoxazole stretching), 1400, 1180  $\text{cm}^{-1}$  ( $-\text{SO}_2-\text{NH}-$  stretching), 925  $\text{cm}^{-1}$  (S–N stretch), 775 (C–Cl stretching), 690 (C–Br stretching);  $^1\text{H NMR}$  (300 MHz, DMSO  $d_6$ ):  $\delta$  7.32 (d, 1H, Ar–H), 7.57 (ddd, 2H, Ar–H), 7.71 (ddd, 2H, Ar–H), 7.79 (d, 1H, Ar–H),



12.7 (s, 1H, 1 × NH). MS (ESI):  $m/z$  = found 421.89 [ $M^+ + 1$ ]; calcd. 419.87.

#### N-(7-methylbenzo[d]oxazol-2-yl)benzene sulfonamide (4)

Yield (%): 60; yellow crystalline solid; m.p.: 174–178 °C; Rf: 0.58 (ethyl acetate/hexane, 5:5); IR (KBr,  $\text{cm}^{-1}$ ): 3150  $\text{cm}^{-1}$  (Ar–H stretching), 1620, 1420  $\text{cm}^{-1}$  (benzoxazole stretching), 1400, 1170  $\text{cm}^{-1}$  (–SO<sub>2</sub>–NH– stretching), 925  $\text{cm}^{-1}$  (S–N stretch); <sup>1</sup>H NMR (300 MHz, DMSO  $d_6$ ):  $\delta$  2.21 (s, 3H, 1 × CH<sub>3</sub>), 7.07 (dd, 1H, Ar–H), 7.46–7.59 (m, 3H, Ar–H), 7.64–7.66 (m, 1H, Ar–H), 7.68–7.77 (m, 3H, Ar–H), 12.8 (s, 1H, 1 × NH). MS (ESI):  $m/z$  = found 289.06 [ $M^+$ ]; calcd. 288.06.

#### 4-methyl-N-(7-methylbenzo[d]oxazol-2-yl)benzene sulfonamide (5)

Yield (%): 69; white crystalline solid; m.p.: 184–188 °C; Rf: 0.63 (ethyl acetate/hexane, 5:5); IR (KBr,  $\text{cm}^{-1}$ ): 3160  $\text{cm}^{-1}$  (Ar–H stretching), 1620, 1420  $\text{cm}^{-1}$  (benzoxazole stretching), 1400, 1150  $\text{cm}^{-1}$  (–SO<sub>2</sub>–NH– stretching), 920  $\text{cm}^{-1}$  (S–N stretch); <sup>1</sup>H NMR (300 MHz, DMSO  $d_6$ ):  $\delta$  2.21 (s, 3H, 1 × CH<sub>3</sub>), 2.33 (s, 3H, 1 × CH<sub>3</sub>), 7.07 (dd, 1H, Ar–H), 7.32 (ddd, 2H, Ar–H), 7.50 (dd, 1H, Ar–H), 7.68–7.74 (m, 3H, Ar–H), 12.8 (s, 1H, 1 × NH). MS (ESI):  $m/z$  = found 303.10 [ $M^+$ ]; calcd. 302.07.

#### 4-bromo-N-(7-methylbenzo[d]oxazol-2-yl)benzene sulfonamide (6)

Yield (%): 66; white solid; m.p.: 194–198 °C; Rf: 0.64 (ethyl acetate/hexane, 5:5); IR (KBr,  $\text{cm}^{-1}$ ): 3160  $\text{cm}^{-1}$  (Ar–H stretching), 1630, 1420  $\text{cm}^{-1}$  (benzoxazole stretching), 1370, 1120  $\text{cm}^{-1}$  (–SO<sub>2</sub>–NH– stretching), 920  $\text{cm}^{-1}$  (S–N stretch), 670 (C–Br stretching); <sup>1</sup>H NMR (300 MHz, DMSO  $d_6$ ):  $\delta$  2.21 (s, 3H, 1 × CH<sub>3</sub>), 7.07 (dd, 1H, Ar–H), 7.46–7.60 (m, 3H, Ar–H), 7.68–7.74 (m, 3H, Ar–H), 12.7 (s, 1H, 1 × NH). MS (ESI):  $M/Z$  = : 369.2 ([ $M^+ + 2$ ], 100%); MS (ESI):  $m/z$  = found 367.87 [ $M^+ + 1$ ]; calcd. 365.97.

#### N-(7-bromobenzo[d]oxazol-2-yl)benzene sulfonamide (7)

Yield (%): 69; white crystalline solid; m.p.: 200–201 °C; Rf: 0.65 (ethyl acetate/hexane, 5:5); IR (KBr,  $\text{cm}^{-1}$ ): 3150  $\text{cm}^{-1}$  (Ar–H stretching), 1630, 1420  $\text{cm}^{-1}$  (benzoxazole stretching), 1370, 1120  $\text{cm}^{-1}$  (–SO<sub>2</sub>–NH– stretching), 930  $\text{cm}^{-1}$  (S–N stretch), 670 (C–Br stretching); <sup>1</sup>H NMR (300 MHz, DMSO  $d_6$ ):  $\delta$  7.41–7.59 (m, 3H, Ar–H), 7.61–7.77 (m, 4H, Ar–H), 7.75 (dd, 1H, Ar–H), 12.7 (s, 1H, 1 × NH). MS (ESI):  $m/z$  = found 352.93 [ $M^+ + 1$ ]; calcd. 351.95.

#### N-(7-bromobenzo[d]oxazol-2-yl)-4-methylbenzenesulfonamide (8)

Yield (%): 60; white crystalline solid; m.p.: 193–198 °C; Rf: 0.54 (ethyl acetate/hexane, 5:5); IR (KBr,  $\text{cm}^{-1}$ ): 3160  $\text{cm}^{-1}$  (Ar–H stretching), 1630, 1420  $\text{cm}^{-1}$  (benzoxazole stretching), 1370, 1120  $\text{cm}^{-1}$  (–SO<sub>2</sub>–NH– stretching), 920  $\text{cm}^{-1}$  (S–N stretch), 680 (C–Br stretching); <sup>1</sup>H NMR (300 MHz, DMSO  $d_6$ ):  $\delta$  2.33 (s, 3H, 1 × CH<sub>3</sub>), 7.32 (ddd, 2H, Ar–H), 7.45 (dd, 1H, Ar–H), 7.66–7.78 (m, 4H, Ar–H), 12.6 (s, 1H, 1 × NH). MS (ESI):  $m/z$  = found 367.22 [ $M^+ + 1$ ]; calcd. 365.97.

#### 4-bromo-N-(7-bromobenzo[d]oxazol-2-yl)benzene sulfonamide (9)

Yield (%): 70; pale-green solid; m.p.: 192–196 °C; Rf: 0.68 acetate/hexane, 5:5); IR (KBr,  $\text{cm}^{-1}$ ): 3150  $\text{cm}^{-1}$  (Ar–H stretching), 1640, 1420  $\text{cm}^{-1}$  (benzoxazole stretching), 1370, 1120  $\text{cm}^{-1}$  (–SO<sub>2</sub>–NH– stretching), 930  $\text{cm}^{-1}$  (S–N stretch), 675 (C–Br stretching); <sup>1</sup>H NMR (300 MHz, DMSO  $d_6$ ):  $\delta$  7.45 (dd, 1H, Ar–H), 7.57 (ddd, 2H, Ar–H), 7.66–7.78 (m, 4H, Ar–H), 12.2 (s, 1H, 1 × NH). MS (ESI):  $m/z$  = found 432.09 [ $M^+ + 2$ ]; calcd. 429.86.

#### N-(benzo[d]oxazol-2-yl)benzene sulfonamide (10)\*

Yield (%): 62; white crystalline solid; m.p.: 211–212 °C (Lit. [35] 210–211 °C); Rf: 0.60 (ethyl acetate/hexane, 5:5); IR (KBr,  $\text{cm}^{-1}$ ): 3160  $\text{cm}^{-1}$  (Ar–H stretching), 1640, 1420  $\text{cm}^{-1}$  (benzoxazole stretching), 1370, 1120  $\text{cm}^{-1}$  (–SO<sub>2</sub>–NH– stretching), 930  $\text{cm}^{-1}$  (S–N stretching); <sup>1</sup>H NMR (300 MHz, DMSO  $d_6$ ):  $\delta$  7.21–7.96 (m, 9H, Ar–H), 12.7 (s, 1H, 1 × NH); MS (ESI):  $m/z$  = found 275.29 [ $M^+$ ]; calcd. 274.04.

#### N-(benzo[d]oxazol-2-yl)-4-methylbenzenesulfonamide (11)\*

Yield (%): 67; white crystalline solid; m.p.: 214–216 °C; Rf: 0.64 (ethyl acetate/hexane, 5:5); IR (KBr,  $\text{cm}^{-1}$ ): 3160  $\text{cm}^{-1}$  (Ar–H stretching), 1640, 1420  $\text{cm}^{-1}$  (benzoxazole stretching), 1370, 1120  $\text{cm}^{-1}$  (–SO<sub>2</sub>–NH– stretching), 930  $\text{cm}^{-1}$  (S–N stretching); <sup>1</sup>H NMR (300 MHz, DMSO  $d_6$ ):  $\delta$  2.35 (s, 3H, 1 × CH<sub>3</sub>), 7.16–7.40 (m, 5H, Ar–H), 7.49 (d, 1H, Ar–H), 7.81 (d, 2H, Ar–H), 12.70 (s, 1H, 1 × NH); MS (ESI):  $m/z$  = found 289.06 [ $M^+$ ]; calcd. 288.06.

#### N-(benzo[d]oxazol-2-yl)-4-bromobenzenesulfonamide (12)

Yield (%): 69; gray crystalline solid; m.p.: 201–202 °C; Rf: 0.61 (ethyl acetate/hexane, 5:5); IR (KBr,  $\text{cm}^{-1}$ ): 3170  $\text{cm}^{-1}$  (Ar–H stretching), 1650, 1420  $\text{cm}^{-1}$  (benzoxazole

stretching), 1370, 1120  $\text{cm}^{-1}$  ( $-\text{SO}_2-\text{NH}-$  stretching), 930  $\text{cm}^{-1}$  (S–N stretching), 635 (C–Br stretching);  $^1\text{H}$  NMR (300 MHz, DMSO  $d_6$ )  $\delta$  7.27–7.38 (m, 2H, Ar–H), 7.54–7.62 (m, 3H, Ar–H), 7.68–7.75 (m, 3H, Ar–H), 12.70 (s, 1H, 1  $\times$  NH). MS (ESI):  $m/z$  = found 353.19 [ $\text{M}^+ + 1$ ]; calcd. 351.95.

#### N-(benzo[d]oxazol-2-yl)-4-nitrobenzenesulfonamide (13)

Yield (%): 72; white crystalline solid; m.p.: 189–191  $^\circ\text{C}$ ; Rf: 0.44 (ethyl acetate/hexane, 5:5); IR (KBr,  $\text{cm}^{-1}$ ): 3170 (Ar–H stretching), 1650, 1420  $\text{cm}^{-1}$  (benzoxazole and  $\text{NO}_2$  stretching), 1370, 1120  $\text{cm}^{-1}$  ( $-\text{SO}_2-\text{NH}-$  stretching), 930  $\text{cm}^{-1}$  (S–N stretching);  $^1\text{H}$  NMR (300 MHz, DMSO  $d_6$ )  $\delta$  7.27–7.38 (m, 2H, Ar–H), 7.59 (ddd, 1H, Ar–H), 7.72 (ddd, 1H, Ar–H), 8.03 (ddd, 2H, Ar–H), 8.10 (ddd, 2H, Ar–H), 12.70 (s, 1H, 1  $\times$  NH). MS (ESI):  $m/z$  = found 320.03 [ $\text{M}^+$ ]; calcd. 319.03.

#### 4-amino-N-(benzo[d]oxazol-2-yl)benzene sulfonamide (14)

Yield (%): 55; white crystalline solid; m.p.: 189–191  $^\circ\text{C}$ ; Rf: 0.44 (ethyl acetate/hexane, 5:5); IR (KBr,  $\text{cm}^{-1}$ ): 3170  $\text{cm}^{-1}$  (Ar–H stretching), 1650, 1420  $\text{cm}^{-1}$  (benzoxazole stretching), 1570 ( $\text{NH}_2$  stretching), 1370, 1120  $\text{cm}^{-1}$  ( $-\text{SO}_2-\text{NH}-$  stretching), 930  $\text{cm}^{-1}$  (S–N stretching);  $^1\text{H}$  NMR (300 MHz, DMSO  $d_6$ )  $\delta$  6.07 (2H, br, s Ar– $\text{NH}_2$ ), 7.02 (ddd, 2H, Ar–H), 7.27–7.38 (m, 2H, Ar–H), 7.59 (ddd, 1H, Ar–H), 7.72 (ddd, 1H, Ar–H), 7.83 (ddd, 2H, Ar–H), 12.70 (s, 1H, 1  $\times$  NH). MS (ESI):  $m/z$  = found 290.31 [ $\text{M}^+$ ]; calcd. 289.05.

#### 5,7-dichloro-2-(1-(phenylsulfonyl)piperidin-4-yl)benzo[d]oxazole (15)

Yield (%): 63; yellow solid; m.p.: 191–194  $^\circ\text{C}$ ; Rf: 0.45 (ethyl acetate/hexane, 6:4); IR (KBr,  $\text{cm}^{-1}$ ): 3170  $\text{cm}^{-1}$  (Ar–H stretching), 2900–2800  $\text{cm}^{-1}$  (piperidine ring stretching), 1650, 1420  $\text{cm}^{-1}$  (benzoxazole stretching), 1182  $\text{cm}^{-1}$  ( $-\text{SO}_2$  stretching), 1108  $\text{cm}^{-1}$  (C–N–C stretching), 750 (C–Cl stretching);  $^1\text{H}$  NMR (300 MHz, DMSO  $d_6$ )  $\delta$  1.67–2.00 (m, 2H, piperidine  $\text{CH}_2$ ), 2.07–2.21 (m, 2H piperidine  $\text{CH}_2$ ), 2.53–2.60 (m, 2H piperidine  $\text{CH}_2$ ), 3.00–3.21 (m, 1H, piperidine CH), 3.56–3.79 (m, 2H, piperidine  $\text{CH}_2$ ), 7.55–7.64 (m, 5H, Ar–H), 7.85–7.88 (m, 2H, Ar–H); MS (ESI):  $m/z$  = found 412.30 [ $\text{M}^+ + 1$ ]; calcd. 410.03.

#### 5,7-Dichloro-2-(1-tosylpiperidin-4-yl)benzo[d]oxazole (16)

Yield (%): 67; white solid; m.p.: 201–204  $^\circ\text{C}$ ; Rf: 0.44 (ethyl acetate/hexane, 6:4); IR (KBr,  $\text{cm}^{-1}$ ): 3270  $\text{cm}^{-1}$  (Ar–H stretching), 2900–2800  $\text{cm}^{-1}$  (piperidine ring stretching), 1650, 1420  $\text{cm}^{-1}$  (benzoxazole stretching), 1170  $\text{cm}^{-1}$  ( $-\text{SO}_2$

stretching), 1108  $\text{cm}^{-1}$  (C–N–C stretching), 760 (C–Cl stretching);  $^1\text{H}$  NMR (300 MHz, DMSO  $d_6$ ):  $\delta$  1.40–1.49 (m, 2H, piperidine  $\text{CH}_2$ ), 1.72–1.78 (m, 2H piperidine  $\text{CH}_2$ ), 2.00–2.31 (m, 2H piperidine  $\text{CH}_2$ ), 2.40 (s, 3H, 1  $\times$   $\text{CH}_3$ ), 2.78–3.00 (m, 1H, piperidine CH), 3.44–3.67 (m, 2H, piperidine  $\text{CH}_2$ ), 7.40–7.42 (m, 2H, Ar–H), 7.61–7.70 (m, 4H, Ar–H); MS (ESI):  $m/z$  = found 426.32 [ $\text{M}^+ + 1$ ]; calcd. 424.04.

#### 2-(1-(4-Bromophenyl)sulfonyl)piperidin-4-yl)-5,7-dichlorobenzo[d]oxazole (17)

Yield (%): 68; white solid; m.p.: 209–211  $^\circ\text{C}$ ; Rf: 0.46 (ethyl acetate/hexane, 6:4); IR (KBr,  $\text{cm}^{-1}$ ): 3260  $\text{cm}^{-1}$  (Ar–H stretching), 2900–2800  $\text{cm}^{-1}$  (Piperidine ring stretching), 1650, 1420  $\text{cm}^{-1}$  (benzoxazole stretching), 1170  $\text{cm}^{-1}$  ( $-\text{SO}_2$  stretching), 1108  $\text{cm}^{-1}$  (C–N–C stretching), 750 (C–Cl stretching), 620 (C–Br stretching);  $^1\text{H}$  NMR (300 MHz, DMSO  $d_6$ ):  $\delta$  1.42–1.49 (m, 2H, piperidine  $\text{CH}_2$ ), 1.72–1.76 (m, 2H piperidine  $\text{CH}_2$ ), 1.98–2.21 (m, 2H piperidine  $\text{CH}_2$ ), 2.78–3.00 (m, 1H, piperidine CH), 3.34–3.62 (m, 2H, piperidine  $\text{CH}_2$ ), 7.35 (d, 1H, Ar–H), 7.56–7.61 (m, 2H, Ar–H), 7.69–7.72 (m, 2H, Ar–H), 7.69 (m, 1H, Ar–H); MS (ESI):  $m/z$  = found 491.19 [ $\text{M}^+ + 3$ ]; calcd. 487.94.

#### 2-(1-(phenylsulfonyl)piperidin-4-yl)benzo[d]oxazole (18)

Yield (%): 68; gray solid; m.p.: 185–187  $^\circ\text{C}$ ; Rf: 0.54 (ethyl acetate/hexane, 6:4); IR (KBr,  $\text{cm}^{-1}$ ): 3260  $\text{cm}^{-1}$  (Ar–H stretching), 2900–2800  $\text{cm}^{-1}$  (Piperidine ring stretching), 1650, 1420  $\text{cm}^{-1}$  (benzoxazole stretching), 1160  $\text{cm}^{-1}$  ( $-\text{SO}_2$  stretching), 1108  $\text{cm}^{-1}$  (C–N–C stretching);  $^1\text{H}$  NMR (300 MHz, DMSO  $d_6$ ):  $\delta$  1.69–1.99 (m, 2H, piperidine  $\text{CH}_2$ ), 2.10–2.30 (m, 2H piperidine  $\text{CH}_2$ ), 2.53–2.60 (m, 2H piperidine  $\text{CH}_2$ ), 2.70–2.75 (m, 1H, piperidine CH), 3.57–3.74 (m, 2H, piperidine  $\text{CH}_2$ ), 7.17–7.46 (m, 1H, Ar–H), 7.52–7.91 (m, 8H, Ar–H); MS (ESI):  $m/z$  = found 343.41 [ $\text{M}^+$ ]; calcd. 342.10.

#### 2-(1-Tosylpiperidin-4-yl)benzo[d]oxazole (19)

Yield (%): 69; gray solid; m.p.: 194–200  $^\circ\text{C}$ ; Rf: 0.64 (ethyl acetate/hexane, 6:4); IR (KBr,  $\text{cm}^{-1}$ ): 3250  $\text{cm}^{-1}$  (Ar–H stretching), 2900–2800  $\text{cm}^{-1}$  (Piperidine ring stretching), 1650, 1420  $\text{cm}^{-1}$  (benzoxazole stretching), 1170  $\text{cm}^{-1}$  ( $-\text{SO}_2$  stretching), 1108  $\text{cm}^{-1}$  (C–N–C stretching);  $^1\text{H}$  NMR (300 MHz, DMSO  $d_6$ ):  $\delta$  1.73–1.94 (m, 2H, piperidine  $\text{CH}_2$ ), 2.08–2.26 (m, 2H piperidine  $\text{CH}_2$ ), 2.48 (s, 3H, 1  $\times$   $\text{CH}_3$ ), 2.55–2.61 (m, 2H piperidine  $\text{CH}_2$ ), 2.98–3.18 (m, 1H, piperidine CH), 3.59–3.72 (m, 2H, piperidine  $\text{CH}_2$ ), 7.09–7.18 (m, 1H, Ar–H), 7.18–7.27 (m, 1H, Ar–H), 7.39–7.50 (m, 1H, Ar–H), 7.63–7.71 (m, 2H, Ar–H), 7.71–7.75 (m, 1H, Ar–H)

7.75–7.83 (m, 2 H, Ar–H); MS (ESI):  $m/z$  = found 357.44 [ $M^+$ ]; calcd. 356.12.

### 2-(1-((4-Bromophenyl)sulfonyl)piperidin-4-yl)benzo[d]oxazole (20)

Yield (%): 80; gray solid; m.p: 201–203 °C; Rf: 0.54 (ethyl acetate/hexane, 6:4); IR (KBr,  $\text{cm}^{-1}$ ): 3250  $\text{cm}^{-1}$  (Ar–H stretching), 2900–2800  $\text{cm}^{-1}$  (piperidine ring stretching), 1650, 1420  $\text{cm}^{-1}$  (benzoxazole stretching), 1160  $\text{cm}^{-1}$  ( $-\text{SO}_2$  stretching), 1108  $\text{cm}^{-1}$  (C–N–C stretching), 630 (C–Br stretching);  $^1\text{H}$  NMR (300 MHz, DMSO  $d_6$ ):  $\delta$  1.67–1.99 (m, 2H, piperidine  $\text{CH}_2$ ), 2.07–2.31 (m, 2H piperidine  $\text{CH}_2$ ), 2.46–2.51 (m, 2H piperidine  $\text{CH}_2$ ), 3.00–3.25 (m, 1H, piperidine CH), 3.56–3.79 (m, 2H, piperidine  $\text{CH}_2$ ), 7.48–7.56 (m, 2H, Ar–H), 7.62–7.70 (m, 4H, Ar–H), 7.76 (d, 1H, Ar–H), 7.94 (d, 1H, Ar–H); MS (ESI):  $m/z$  = found 422.31 [ $M^+ + 1$ ]; calcd. 420.01.

\*Compounds known in the literature [25, 26]

## Molecular docking studies

It will provide up-front information that can also be used for structural optimization. Molecular modeling is a computer-based process for the derivation, demonstration and manipulation of molecular entities and their reactions. It has been used to understand many of the three-dimensional structure-dependent properties.

The 3D structures were created by using the SKETCH module employed in the SYBYL-X 2.0 program (Tripos Associates, St. Louis, MO, USA) [27]. Using the standard Tripos force field, Clark et al. [28] the geometry optimization was applied with a distance-dependent dielectric function at the convergence gradient of 0.001 kcal/mol. Utilizing MMFF94 (Merck Molecular Force Field) the electrostatic charges were calculated.

Utilizing the in-built program of SYBYL-X 2.0, structures were subjected to molecular dynamic simulation, to perform conformational analysis. Using the repeated molecular dynamics, molecules were heated to 1000 K for 2000 fs (2 ps) and annealed slowly to 0 K in a step of 100 K for 1000 fs at each temperature, utilizing an exponential annealing function. By following this process, 100 conformations were sampled out throughout 100 cycles which accounted for conformational flexibility with the least energy and stable conformations.

Surflex-Dock, a patented search engine, which is coupled with a unique scoring function, was adopted Jain et al. [29, 30] for molecular docking. The crystal structure of *M. tuberculosis inhA*, the enoyl acyl carrier protein reductase (ENR) complexed with 1-cyclohexyl-N-(3, 5-dichlorophenyl)-5-oxopyrrolidine-3-carboxamide (PDB ID 4TZK, 1.62 Å X-ray

resolution) was extracted from the Brookhaven Protein Database (PDB <http://www.rcsb.org/pdb>). [22].

In our docking procedure, water molecules and other ligands in the crystal structures were removed (except cofactor NAD+). Polar hydrogen atoms with Gasteiger-Huckel charges Gasteiger et al. [31] were added. Then, the ligand-based mode was adopted to generate the “protomol,” by fixing the threshold and bloat parameters with their default values of 0.50 and 0 Å. After these procedures, benzoxazole derivatives were docked within the prepared protein. In the crystal structure of 1-cyclohexyl-N-(3, 5-dichlorophenyl)-5-oxopyrrolidine-3-carboxamide-*inhA* (4TZK PDB) domain, the mode of collaboration of the relative ligands has been used as the standard docked template. While performing the molecular docking studies, the maximum number of orientations per ligand was fixed to 20 without restraints.

Based on three selection criteria, the docking complex was acknowledged,

- (i) Highest docking score should represent docking score of the best orientation
- (ii) Alignment of the aromatic/aliphatic rings of the our molecules (ligands) into the active site in a comparable fashion with the cocrystallized ligands orientation
- (iii) Conservation of two major key interactions, i.e., H-bonds with cofactor NAD+ and amino acid residue Tyr158

In order to predict the binding affinity of the designed molecules in the relative analysis, score functions, i.e., D Score Kuntz et al. [32], PMF score Muegge and Martin [33], Chem score Eldridge et al. [34] and Score Jones et al. [35], were estimated using C-Score module in SYBYL-X 2.0.

## Antimycobacterial assay

Using microplate alamarBlue assay (MABA), antimycobacterial activity of the synthesized compounds was evaluated against *M. tuberculosis* Lourenço et al. [36]. In order to reduce background effect, assay was executed in 96-well microplates with black and clear bottom. In this assay, 200  $\mu\text{l}$  of autoclaved deionized water was supplemented to all external perimeter wells of sterile 96-well plates, to reduce evaporation of culture medium in the test wells during incubation. In the 96-well plates, 100  $\mu\text{l}$  of the middle brook 7H9 culture broth was added and serial dilutions of compounds were performed in the microplate and finally 0.2  $\mu\text{g}/\text{ml}$  to 100  $\mu\text{g}/\text{ml}$  drug concentrations were selected for the assay. Microplates were incubated at 37°C for five days. Meanwhile, 25  $\mu\text{l}$  of fresh 1:1 mixture of alamarBlue reagent and 10% Tween 80 was added to the plate and incubated for 24 h. Blue color in the well indicates no bacterial growth, and pink color was

interpreted as bacterial growth. Pyrazinamide (3.125 µg/ml), ciprofloxacin (3.125 µg/ml) and streptomycin (6.25 µg/ml) were used as standards. The MIC was defined as the lowest drug concentration which prevented the color change from blue to pink. The vaccine strain *Mycobacterium tuberculosis* H37Rv (ATCC No-27294) was used in this assay.

### In silico prediction of human cell line cytotoxicity for benzoxazole derivatives

CLC-Pred (cell line cytotoxicity predictor) is a freely available web service which was utilized for in silico cytotoxic effect prediction of chemical compounds in non-transformed and cancer cell lines Lagunin et al. [24]. CLC-Pred is a very useful tool in the prediction of cytotoxicity of organic compounds to evaluate the significance of the chemical substance's inclusion in cytotoxic experimental screening cascade.

The prediction relies on the technology, viz. Prediction of Activity Spectra for Substances (PASS) (<http://www.way2drug.com/PASSonline>). Training set was produced on the basis of cytotoxicity data salvaged from ChEMBLdb (version 23) (<https://www.ebi.ac.uk/chembl/db/>).

The prediction results were displayed in two tables, one for tumor and another for nontumor (normal) cell lines. Table contains details of cytotoxicity with short or full names of the cell lines, along with corresponding names of the tissue or organs. Each table includes the Pa (probability "to be active") and Pi (probability "to be inactive") values. The predictive parameter generated, viz. the Pa values (probability "to be active"), is categorized as "active" if the values are > 0.5 with the projected cancer cell line. If Pa value is < 0.5 for the set compounds, then the probabilities of being cytotoxic to the mentioned cell lines are less.

Additional investigations on benzoxazole scaffolds are under active investigations and will be communicated in the future.

**Acknowledgements** The authors thankfully acknowledge Dr KG Bhat, Maratha Mandal's Dental College, Hospital and Research Centre, Belgaum, India, for antitubercular tests. The authors are grateful to Shrinivas D. Joshi, Professor and Head, Department of Pharmaceutical Chemistry, S.E.T's College of Pharmacy, Dharwad, India, for docking studies.

### References

1. E. Bogatcheva, C. Hanrahan, B. Nikonenko, Identification of new di amine scaffolds with activity against *Mycobacterium tuberculosis*. *J. Med. Chem.* **49**, 3045–3048 (2006). <https://doi.org/10.1021/jm050948+>
2. A. Rattan, A. Kalia, N. Ahmad, Multidrug-resistant *Mycobacterium tuberculosis*: molecular perspectives. *Emerg. Infect. Dis.* **4**, 195–209 (1998). <https://doi.org/10.3201/eid0402.980207>
3. N. Qureshi, N. Sathyamoorthy, K. Takayama, Biosynthesis of C<sub>30</sub> to C<sub>56</sub> fatty acids by an extract of *Mycobacterium tuberculosis* H37Rv. *J. Bacteriol.* **157**, 46–52 (1984)
4. K. Bloch, Control mechanisms for fatty acid synthesis in *Mycobacterium Smegmatis*. *Science* (1977). <https://doi.org/10.1002/9780470122907.ch1>
5. S. Kikuchi, D.L. Rainwater, P.E. Kolattukudy, Purification and characterization of an unusually large fatty acid synthase from *Mycobacterium tuberculosis* var. bovis BCG. *Arch. Biochem. Biophys.* **295**, 318–326 (1992). [https://doi.org/10.1016/0003-9861\(92\)90524-z](https://doi.org/10.1016/0003-9861(92)90524-z)
6. M.C. Lourenco, M.V. de Souza, A.C. Pinheiro, M.D.L. Ferreira, R.S. Gonçalves, T.C.M. Nogueira, M.A. Peralta, Evaluation of anti-Tubercular activity of nicotinic and isoniazid analogues. *Arxivoc* **15**, 181–191 (2007)
7. N.C. Desai, A. Trivedi, H. Somani, K.A. Jadeja, D. Vaja, L. Nawale, D. Sarkar, Synthesis, biological evaluation, and molecular docking study of pyridine clubbed 1, 3, 4-oxadiazoles as potential antituberculars. *Synth. Commun.* **48**, 524–540 (2018). <https://doi.org/10.1080/00397911.2017.1410892>
8. M. Martínez-Hoyos, E. Perez-Herran, G. Gulten, L. Encinas, D. Álvarez-Gómez, E. Alvarez, J. Rullas-Trincado, Antitubercular drugs for an old target: GSK693 as a promising *inhA* direct inhibitor. *EbioMedicine* **8**, 291–301 (2016). <https://doi.org/10.1016/j.ebiom.2016.05.006>
9. U. Kamal, N.M. Javed, K. Arun, Biological potential of benzoxazole derivatives: an updated review. *Asian J. Pharm. Clin. Res.* **13**, 28–41 (2020). <https://doi.org/10.22159/ajpcr.2020.v13i8.37958>
10. A. Kumar, D. Kumar, Synthesis and antimicrobial activity of metal complexes from 2-(1/2'-hydroxynaphthyl) benzoxazoles. *Arxivoc* **10**, 399 (2007). <https://doi.org/10.3998/ark.5550190.0008.e12>
11. Y. Katsura, Y. Inoue, S. Nishino, M. Tomoi, H. Itoh, H. Takasugi, Studies on antiulcer drugs. III. Synthesis and antiulcer activities of imidazo[1,2-a]pyridinylethyl benzoxazoles and related compounds. A novel class of histamine H<sub>2</sub>-receptor antagonists. *Chem. Pharm. Bull.* **40**, 1424–1438 (1992). <https://doi.org/10.1248/cpb.40.1424>
12. R.D. Haugwitz, R.G. Angel, G.A. Jacobs, B.V. Maurer, V.L. Narayanan, L.R. Cruthers, J. Szanto, Synthesis and anthelmintic activities of novel 2- heteroaromatic-substituted isothiocyanato benzoxazoles and benzothiazoles. *J. Med. Chem.* **25**, 969–974 (1982). <https://doi.org/10.1021/jm00350a017>
13. C.J. Paget, K. Kisner, R.L. Stone, D.C. DeLong, Heterocyclic substituted ureas. II. Immunosuppressive and antiviral activity of benzothiazole- and benzoxazoleureas. *J. Med. Chem.* **12**, 1016–1018 (1969). <https://doi.org/10.1021/jm00306a011>
14. O. Temiz-Arpaci, I. Yildiz, S. Ozkan, F. Kaynak, E. Aki-Sener, I. Yalçin, Synthesis and biological activity of some new benzoxazoles. *Eur. J. Med. Chem.* **43**, 1423–1431 (2008). <https://doi.org/10.1016/j.ejmech.2007.09.023>
15. Z.A. Bhavsar, P.T. Acharya, D.J. Jethava, H.D. Patel, Recent advances in development of anthelmintic agents: synthesis and biological screening. *Synth. Commun.* **50**, 917–946 (2020). <https://doi.org/10.1080/00397911.2019.1695276>
16. V. Šlachtová, L. Brulíková, Benzoxazole derivatives as promising antitubercular agents. *Chem. Select* **3**, 4653–4662 (2018). <https://doi.org/10.1002/slct.201800631>
17. T. Ertan-Bolelli, I. Yildiz, S. Ozgen-Ozgacar, Synthesis, molecular docking and antimicrobial evaluation of novel benzoxazole derivatives. *Med. Chem. Res.* (2016). <https://doi.org/10.1007/s00044-015-1499-1>
18. S. Joshi, U. More, S. Sorathiya, D. Koli, T. Aminabhavi, Pyrrolyl thiadiazoles as *Mycobacterium tuberculosis* inhibitors and their *In silico* analyses. *Annu. Rep. Med. Chem.* **5**, 1–20 (2015). <https://doi.org/10.2147/RRMC.S80395>

19. S.D. Joshi, S.R. Dixit, J. Basha, V.H. Kulkarni, T.M. Aminabhavi, M.N. Nadagouda, C. Lherbet, Pharmacophore mapping, molecular docking, chemical synthesis of some novel pyrrolyl benzamide derivatives and evaluation of their inhibitory activity against enoyl-ACP reductase (*inhA*) and *Mycobacterium tuberculosis*. *Bioorg. Chem.* **81**, 440–453 (2018). <https://doi.org/10.1016/j.bioorg.2018.08.035>
20. A. Gaulton, A. Hersey, M. Nowotka, A.P. Bento, J. Chambers, D. Mendez, M. Davies, The ChEMBL database in 2017. *Nucleic Acids Res.* **45**, 945–954 (2017). <https://doi.org/10.1093/nar/gkw1074>
21. Y. Wang, S.H. Bryant, T. Cheng, J. Wang, A. Gindulyte, B.A. Shoemaker, J. Zhang, PubChem BioAssay: 2017 update. *Nucleic Acids Res.* **2017**(45), D955–D963 (2017). <https://doi.org/10.1093/nar/gkw1118>
22. <http://www.rcsb.org/pdb>
23. X. He, A. Alian, R. Stroud, Ortiz de Montellano PR Pyrrolidine carboxamides as a novel class of inhibitors of enoyl acyl carrier protein reductase from *Mycobacterium tuberculosis*. *J. Med. Chem.* **21**, 6308–6323 (2006). <https://doi.org/10.1021/jm060715y>
24. A.A. Lagunin, V.I. Dubovskaja, A.V. Rudik, P.V. Pogodin, D.S. Druzhilovskiy, T.A. Glorizova, V.V. Poroikov, CLC-Pred: a freely available web-service for *In silico* prediction of human cell line cytotoxicity for drug-like compounds. *PLoS one* **13**, e0191838 (2018). <https://doi.org/10.1371/journal.pone.0191838>
25. H. Zali-Boeini, Z. Najafi, One-step synthesis ofazole- and benzazole-based sulfonamides in aqueous media. *Mol. Divers.* **19**, 283–292 (2015). <https://doi.org/10.1007/s11030-015-9567-5>
26. Z.B. Shi, D. Zhao, Y.Y. Huang, Y. Du, X.R. Cao, Z.N. Gong, J.X. Li, Discovery, synthesis and evaluation of small-molecule signal transducer and activator of transcription 3 inhibitors. *Chem. Pharm. Bull.* **60**, 1574–1580 (2012). <https://doi.org/10.1248/cpb.c12-00745>
27. Tripos International (2012) SYBYL-X 2.0, Tripos International, St. Louis, MO, USA
28. M. Clark, R.D. Cramer, N. Van Opdenbosch, Validation of the general purpose Tripos 5.2 force field. *J. Comput. Chem.* **10**, 982–1012 (1989). <https://doi.org/10.1002/jcc.540100804>
29. A.N. Jain, Scoring non covalent protein-ligand interactions: a continuous differentiable function tuned to compute binding affinities. *J. Comput. Aided Mol. Des.* **10**, 427–440 (1996). <https://doi.org/10.1007/BF00124474>
30. A.N. Jain, Surflex: fully automatic flexible molecular docking using a molecular similarity-based search engine. *J. Med. Chem.* **46**, 499–511 (2003). <https://doi.org/10.1021/jm020406h>
31. J. Gasteiger, M. Marsili, Iterative partial equalization of orbital electronegativity a rapid access to atomic charges. *Tetrahedron* **36**, 3219–3228 (1980). [https://doi.org/10.1016/0040-4020\(80\)80168-2](https://doi.org/10.1016/0040-4020(80)80168-2)
32. I.D. Kuntz, J.M. Blaney, S.J. Oatley, R. Langridge, T.E. Ferrin, A geometric approach to macromolecule-ligand interactions. *J. Mol. Biol.* **161**, 269–288 (1982). [https://doi.org/10.1016/0022-2836\(82\)90153-x](https://doi.org/10.1016/0022-2836(82)90153-x)
33. I. Muegge, Y.C. Martin, A general and fast scoring function for protein-ligand interactions: a simplified potential approach. *J. Med. Chem.* **42**, 791–804 (1999). <https://doi.org/10.1021/jm980536j>
34. M.D. Eldridge, C.W. Murray, T.R. Auton, G.V. Paolini, R.P. Mee, Empirical scoring functions: I. The development of a fast empirical scoring function to estimate the binding affinity of ligands in receptor complexes. *J. Comput. Aided Mol. Des.* **11**, 425–445 (1997). <https://doi.org/10.1023/a:1007996124545>
35. G. Jones, P. Willett, R.C. Glen, A.R. Leach, R. Taylor, Development and validation of a genetic algorithm for flexible docking. *J. Mol. Biol.* **267**, 727–748 (1997). <https://doi.org/10.1006/jmbi.1996.0897>
36. R.S. Reis, I. Neves, S.L. Lourenço, L.S. Fonseca, M.C.S. Lourenço, Comparison of flow cytometric and Alamar Blue tests with the proportional method for testing susceptibility of *Mycobacterium tuberculosis* to rifampin and isoniazid. *J. Clin. Microbiol.* **42**, 2247–2248 (2004). <https://doi.org/10.1128/jcm.42.5.2247-2248.2004>